Kinetic Monte Carlo simulations of binary alloy film growth

1999 J. Phys.: Condens. Matter 11 10007

(http://iopscience.iop.org/0953-8984/11/49/318)

J. Phys.: Condens. Matter **11** (1999) 10007–10018. Printed in the UK PII: S0953-8984(99)04727-X

Kinetic Monte Carlo simulations of binary alloy film growth

Y Shim†, D P Landau† and S Pal‡

† Center for Simulational Physics, University of Georgia, Athens, GA 30602, USA
‡ 104 Davey Laboratory, Department of Physics, The Pennsylvania State University, University Park, PA 16802, USA

Received 2 June 1999

Abstract. Using kinetic Monte Carlo simulations of film growth with simple models, we have examined $A_{0.5}B_{0.5}$ film growth in 2 + 1 dimensions and have compared it with new results for monatomic film growth. On the basis of data on the domain size, long-range order in each layer *l*, and surface fluctuations we examine the dynamic relation between surface-induced domain growth and growth-induced surface roughening.

1. Introduction

One of the great developments of the 21st century will surely be the rise of 'designer' materials, often on the nanoscale or mesoscale. It is thus clear that the understanding of the nature of film growth by modern methods such as molecular beam epitaxy (MBE) presents an important challenge from both fundamental and technological perspectives. Furthermore, it is likely that a combination of experiment, theory, and computer simulation will be needed to produce the requisite understanding. Many studies have already been made in an attempt to understand growth-induced surface roughening and the underlying mechanisms of thin-film growth [1, 2], but most often only simple discrete models of homoepitaxial film growth have been simulated, primarily to study surface fluctuations, structure factors, and height–height correlations. Phenomenological continuum growth equations have been also derived from symmetry arguments and analysed by renormalization group methods or numerical calculations; however, detailed mechanisms of binary alloy (A_xB_{1-x}) film growth and consequences of surface roughening processes are less well understood. There have been experimental observations of atomic ordering in alloy films of $Si_{1-x}Ge_x$ [3], $Al_xGa_{1-x}As$ [4], $Ga_xIn_{1-x}As$ [5], and $Ga_xIn_{1-x}P$ [6,7] grown by epitaxial techniques. The degree of long-range order observed in the experiments is strongly affected by the properties of the materials used and epitaxial conditions (e.g., surface temperature [3, 8], growth rate [9]).

Experiments indicate that the ordering takes place near the surface exposed to the incoming particle-beam flux and show that the presence of the long-range order (LRO) is mainly due to surface phenomena and cannot be explained by the bulk or equilibrium properties. The ordering is a metastable state which is irreversibly destroyed by annealing although it is sustained up to a rather high temperature if bulk diffusion is negligible [3]. Thus, one interesting question is that of how growth-induced atomic ordering in metallic alloys [10, 11] and compound semiconductors [3–5, 8, 12] is related to the growth-induced surface roughening process during the film growth. A kinetic mean-field calculation [13, 14] shows that the morphology of the films affects the evolution of the LRO. Simulations of a (1 + 1)-dimensional binary alloy model

0953-8984/99/4910007+12$30.00

also show the interplay between pattern formation and kinetic roughening [15]. The scaling result of surface roughness in the growth of $Si_{1-x}Ge_x$ on Si [16] indicates that at large length scales surface morphology is well described by Edwards–Wilkinson (EW) [17] behaviour.

Here we report the results of the surface-induced domain growth and the growth-induced surface roughening for a simple model of binary alloy films grown by molecular beam epitaxy (MBE) simulations. We do not attempt to include full physical complexity but deal with rather simple models which we hope will exhibit the essential features of the system.

2. Background

A theoretical description of pattern formation for the case of a non-conserved order parameter (NCOP) is known as model A [18]. Experiments and theoretical studies for the NCOP [19,20] show that the average domain size $R(t)$ grows as a power law in time, i.e.,

$$R(t) \sim t^{\phi} \tag{1}$$

where $\phi = 1/2$ is the characteristic exponent. On the other hand, for the case of a conserved scalar order parameter, the exponent $\phi = 1/3$. The structure factor $S_D(k, t)$ for domain growth is defined as

$$S_D(\boldsymbol{k}, t) = (1/L^d) \sum_{\boldsymbol{r}} \langle \psi(\boldsymbol{r}, t)\psi(0, t)\rangle \, e^{-i\boldsymbol{k}\cdot\boldsymbol{r}} = R(t)^d s_D(kR(t)) \tag{2}$$

in d dimensions, where $\psi(\boldsymbol{r}, t)$ is the local order parameter, $\boldsymbol{k}$ is a wave vector with $k = |\boldsymbol{k}|$, L is the lateral system size, and $s_D(kR(t))$ is a scaling function. For a NCOP the mean square domain size can be simply defined as

$$R^2(t) = \left\langle \frac{1}{N} \left[\sum_{\boldsymbol{r}}^{N} \psi(\boldsymbol{r}, t) \right]^2 \right\rangle \tag{3}$$

with total number of particles N, which corresponds to the $k = 0$ peak of $S_D(\boldsymbol{k}, t)$ [21].

The growth-induced surface roughening of a growing film is usually characterized by the interfacial width

$$w(L, t) = \left\langle [h(\boldsymbol{r}, t) - \langle h(t)\rangle]^2 \right\rangle^{1/2} \sim L^{\zeta} f(t/L^z) \tag{4}$$

where $h(\boldsymbol{r}, t)$ is the height at lateral position $\boldsymbol{r}$ and time t and

$$\langle h(t)\rangle = (1/L^2) \sum_{\boldsymbol{r}} h(\boldsymbol{r}, t).$$

ζ and z in the scaling form [22] given in equation (4) are the roughness and dynamic exponent, respectively. The scaling function $f(x) \sim x^{\zeta/z}$ for $x \ll 1$ and approaches a constant for $x \gg 1$. For $1 \ll t \ll L^z$, $w(t) \sim t^{\beta}$ with the growth exponent $\beta = \zeta/z$, and the lateral correlation length $\xi(t) \sim t^{1/z}$. The structure factor

$$S(\boldsymbol{k}, t) = (1/L^{d'}) \sum_{\boldsymbol{r}} \left[\langle h(\boldsymbol{r}, t)h(0, t)\rangle - \langle h(t)\rangle^2 \right] e^{-i\boldsymbol{k}\cdot\boldsymbol{r}} \sim k^{-\gamma} s(k^z t) \tag{5}$$

and the scaling form given in equation (5) is valid in the long-wavelength limit with $\gamma = 2\zeta + d'$, where d' ($d' = d - 1$) is the substrate dimension. The scaling function $s(x) \sim$ constant for $x \gg 1$ and in the case of $x \ll 1$, $s(x) \sim x$ for $\gamma \geqslant z$ and $s(x) \sim x^{\gamma/z}$ for $\gamma \leqslant z$ [23]. Thus, the saturated structure factor is $S(k) \sim k^{-\gamma}$ with $\gamma = z$ if the growth process can be described by a Langevin equation. When the surface mass current is $\boldsymbol{J} = -\nu \boldsymbol{\nabla} h$, one obtains the EW equation, $\partial h/\partial t = \nu \nabla^2 h + \eta$, which yields $\zeta = 0$ and $z = 2$ in $d' = 2$ dimensions [17]. If the main relaxation process is surface diffusion, i.e., $\boldsymbol{J} \propto \boldsymbol{\nabla}(\nabla^2 h)$, then one can obtain

Mullins–Herring (MH) equation, $\partial h/\partial t = -\kappa\,\nabla^4 h + \eta$ [24] with $\zeta = 1$ and $z = 4$ in $d' = 2$ dimensions [25]. It has been suggested that the hyperscaling relation [26]

$$z = 2\zeta + d' \tag{6}$$

holds for any growth model described by the continuum Langevin equation.

3. Model and method

The simplest situation in heteroepitaxial film growth is when A-type material grows on a substrate of material B as in the growth of Ge on a Si substrate. For simplicity, in the following we shall ignore the lattice mismatch between the substrate and the growing adlayer. In molecular beam epitaxy (MBE), particles are randomly deposited at a given rate (F), in units of monolayers per second (ML s^{-1}), on an initially flat substrate maintained with a fixed temperature (T) and then diffuse around the surface; the diffusion rate (D) denotes the number of attempts at surface diffusion per site per second. In our kinetic Monte Carlo MBE simulations, we consider a $(2+1)$-dimensional simple solid-on-solid model in which the substrate is an $L \times L$ square lattice with periodic boundary conditions. Vacancies, overhangs, and desorption from the surface are not allowed. For binary alloy film growth, the deposition rate of A-type particles is xF, while for B it is $(1-x)F$, where x is the concentration of A particles. We have used an A-type substrate to mimic the growth of $Si_{1-x}Ge_x$ on Si and deposited A and B particles with equal probability, i.e., we restrict ourselves to $x = 0.5$.

A particle is randomly chosen for surface diffusion after random deposition of A and B particles according to the flux F and the concentration x. The probability(P_H) of some diffusion event occurring is given by

$$P_H = \exp\left[-E(A,B)/k_B T\right] \tag{7}$$

where a site-dependent activation energy $E(A,B)$ is determined by the local configurations of bonding between the nearest neighbours, i.e., $E(A,B) = n_{AA}J_{AA} + n_{BB}J_{BB} + n_{AB}J_{AB}$ where n_{AA}, n_{BB}, and n_{AB} are the number of A–A, B–B, and A–B pairs with nearest neighbours, respectively. J_{AA}, J_{BB}, and J_{AB} are effective A–A, B–B, and A–B bond energies.

After breaking the bonds, depending upon the model used, a particle at the mth site may either diffuse randomly including moving up or down (UDR model) with the constant transition probability $P_D = 1/4$ to any of the nearest-neighbour sites, or diffuse randomly to a nearest-neighbour kth site with the preferential probability (UDP model)

$$P_D(m \to k) \propto \exp\left[E_k(A,B)/k_B T\right] \tag{8}$$

where $E_k(A,B)$ is the binding energy available at the kth site. In order to study atomic ordering observed in a variety of binary alloy films, we have used antiferromagnetic-like effective interactions. In a preferential binary alloy (PBA) model, we used the interactions $(J_{AA}, J_{BB}, J_{AB}) = (0.3, 0.3, 1)J$, but in a restricted preferential binary alloy (PBA) model in which particles hop up no more than one lattice constant, we used the interactions $(J_{AA}, J_{BB}, J_{AB}) = (-1, -1, 1)J$, where $J > 0$. We have also considered a random binary alloy (RBA) model, which is an UDR model, with the same interactions as in the PBA model, to see the effect of a change in a diffusion rule. Thus, an A-type (B-type) particle tends to make a bond with a B-type (A-type) particle due to those interactions. Note that when the concentration $x = 1$, the PBA and RBA models correspond to monatomic UDP and UDR models, respectively. The first homoepitaxial version was reported in EWSSW94 for the down preferential (DP) and UDP models [27], and we now extend the calculations to consider the case of random diffusion and to the treatment of binary alloy film growth, hoping to capture the

essential features of the non-equilibrium behaviour of domain growth and surface roughening. We do not expect these simple models to provide a quantitative description of a physical alloy film.

The growing binary alloy model can be described in terms of a spin-1 Ising model [28]. Thus, if the $\boldsymbol{r}$-site at a layer number l is occupied by an A (B) atom at time t, then $\sigma(\boldsymbol{r}, l) = 1\ (-1)$. Otherwise the site is empty and $\sigma(\boldsymbol{r}, l) = 0$. There are many site updatings due to the deposition and diffusion, so all the spin configurations inside the bulk must be recorded. After the long-range order (LRO) reaches its asymptotic value, we turned off the flux and quenched the system. The quenched LRO and the mean square quenched order are defined as

$$M(l) = \left\langle \frac{1}{L^2} \left| \sum_{\boldsymbol{r}} (-1)^r \sigma(\boldsymbol{r}, l) \right| \right\rangle \tag{9}$$

$$M^2(l) = \left\langle \left[\frac{1}{L^2} \sum_{\boldsymbol{r}} (-1)^r \sigma(\boldsymbol{r}, l) \right]^2 \right\rangle \tag{10}$$

where

$$\sum_{\boldsymbol{r}} (-1)^r = \sum_{i=1}^{L} \sum_{j=1}^{L} (-1)^{i+j}$$

with $\boldsymbol{r} = i\hat{x} + j\hat{y}$ and $\sigma(\boldsymbol{r}, l)$ can be 1 (or -1) if an A (or B) atom occupies the site because of the assumption of no overhangs and no vacancies. The definition of the LRO is equivalent to that of the staggered magnetization in a magnetic system. The mean square quenched order $M(l)^2$ has been calculated up to the maximum layer number l_m for which the layer is entirely filled.

It has been shown [29] that the domain size at the layer number l may be defined as the $k = 0$ peak of structure factor $S_{\mathrm{D}}(\boldsymbol{k}, l)$, i.e., $S_{\mathrm{D}}(0, l)$, where

$$S_{\mathrm{D}}(\boldsymbol{k}, l) = (1/L^2) \sum_{\boldsymbol{r}} \langle \psi(\boldsymbol{r}, l) \psi(0, l) \rangle \, \mathrm{e}^{-\mathrm{i}\boldsymbol{k}\cdot\boldsymbol{r}}$$

with $\psi(\boldsymbol{r}, l) = (-1)^r \sigma(\boldsymbol{r}, l)$. In analogy to equation (3), we define the mean square domain size as

$$R^2(l) = L^2 M^2(l). \tag{11}$$

The domain size $R(l)$ is also related to the domain growth exponent z_{D} at late times:

$$R(l) \sim l^{1/z_{\mathrm{D}}} \tag{12}$$

based on the self-similar behaviour of the domain growth.

Simulations have been carried out for $10 \leqslant L \leqslant 160$ with the different number of layers grown depending on the system size L using IBM RS6000 and Pentium workstations. The growth was repeated with different random numbers and results were averaged to reduce the statistical errors.

4. Results

4.1. Results for homoepitaxial growth

The behaviour of the monatomic UDP model appears to be the same as for the atomistic version of the Edwards–Wilkinson model, i.e. the growth of the interfacial width is logarithmic with time, and the dynamic exponent is $z = 1.6$ for the data shown in figure 1(a). The behaviour

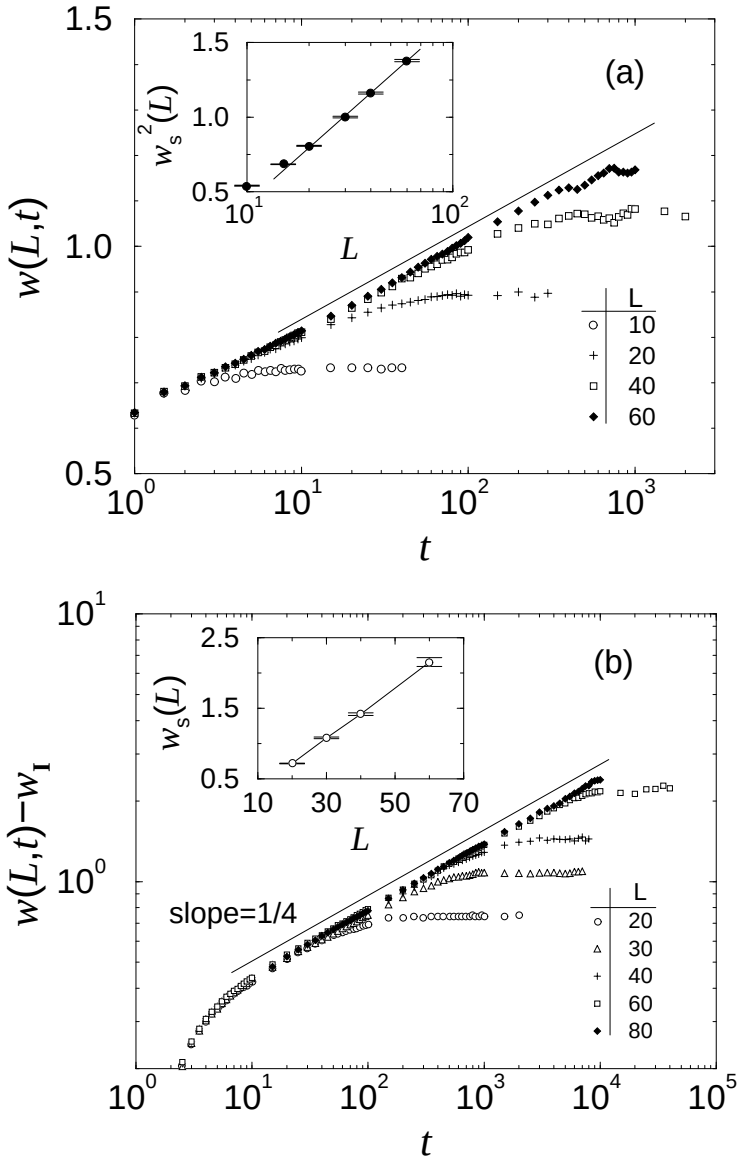

Figure 1. (a) Variation of the interfacial width with time for the monatomic UDP model. The solid line is a guide with $w(t) \sim \log t$. The inset shows $w_s^2(L) \sim \log L$. (b) Variation of the interfacial width with time for the monatomic UDR model. The inset shows $w_s(L) = aL + w_I$ with $a = 0.37$ and $w_I = 0.86$. In both figures $k_B T/J = 1.0$, $F = 1$ ML s^{-1}, and $D = 100$ s^{-1}/site.

of the saturated mean square width varies logarithmically with the size L (see the inset). In the monatomic UDP model, a particle prefers a site in a valley on the surface to one atop a hill because such a site provides more chances to increase the number of bonds with nearest neighbours for the particle. This preferential movement results in a downhill current and leads to EW behaviour. The behaviour of the monatomic UDR model for the same growth conditions turns out to be quite different. As shown in figure 1(b), the growth obeys a power law with $\beta = 1/4$ and the dynamic exponent $z = 4$. The saturated interfacial width $w_s(L) \sim L$,

which means means that $\zeta = 1$ and surface diffusion is the main relaxation process. The saturated structure factor $S(k) \sim k^{-\gamma}$ and its scaling collapse yields $\gamma = 4$ with $z = \gamma$ for the monatomic UDR model.

4.2. Binary alloy growth: domain formation

The results of domain growth for the restricted PBA model are consistent with the Allen–Cahn theory [30] for a NCOP. According to the theory, the normal velocity of a curved antiphase boundary (APB) is linearly proportional to the mean curvature. The motion of the APB evolves in such a way as to reduce the curvature in order to minimize surface tension by bulk diffusion. In the case of domain growth by MBE, the pattern of ordered domains and antiphase boundaries at early times affects the morphology of growing films and the average size of ordered clusters. The layer number dependence of the motion of the APB shows non-trivial behaviour due to the surface roughening and competition between ordering and disordering by thermal fluctuations.

Figure 2 shows vertical cross sections of a film after deposition of 320 layers. The rough surface can be seen in this figure; the ordered domain size grows and the streaks of APBs extend vertically from the substrate to the surface. Some of APBs, which have a parabolic shape, are eliminated by the coarsening process. These are in good agreement with experiments [6, 7, 9] and simulations of the CuPt type of ordering [31, 32]. Horizontal cross sections of the same grown film indicate that the density of APBs decreases as the layer number l increases, which

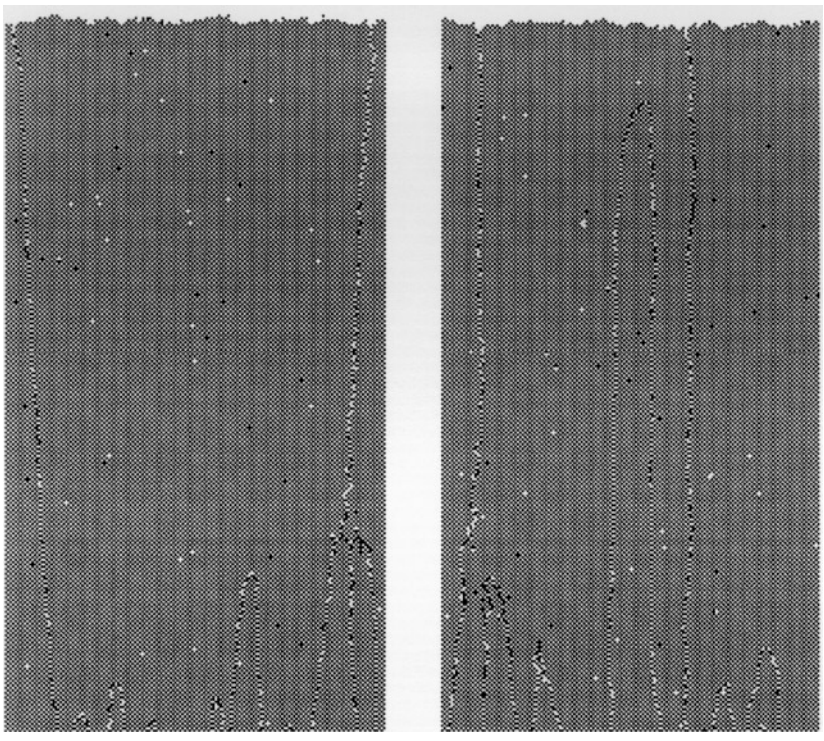

(a) (b)

Figure 2. Vertical cross sections of a film after deposition of 320 layers for the restricted PBA model. Here, $L = 160$, $k_B T/J = 1.0$, $F = 1$ ML s^{-1}, and $D = 80$ s^{-1}/site. A white (black) square is an A (B) adatom. The two vertical cross sections are perpendicular to each other.

means that the magnitude of LRO also increases as films grow due to the coarsening process before finally saturating because of a finite size of the substrate.

Figure 3(a) shows the mean square domain size $R^2(l)$ for the restricted PBA model. The solid line in figure 3(a) is a power-law fit for $L = 80$ and for large $l \geqslant 200$:

$$R^2(l) \sim l. \tag{13}$$

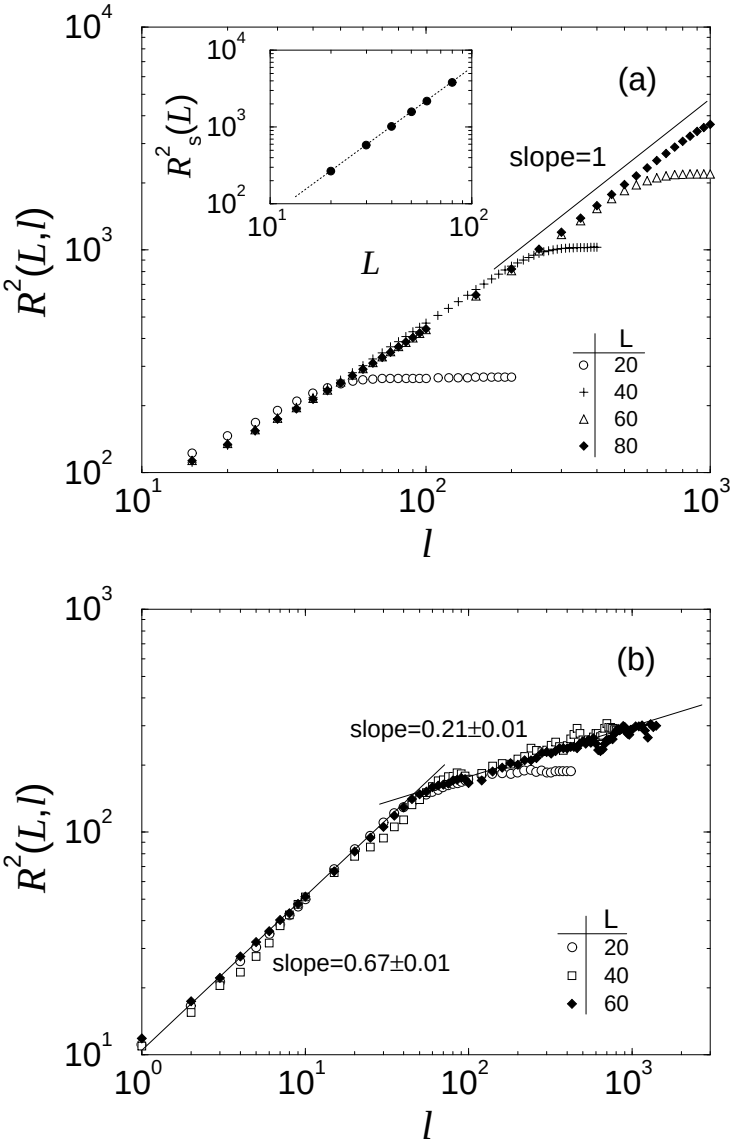

Figure 3. (a) The mean square domain size $R^2(l)$ for the restricted PBA model as a function of the layer number l for $20 \leqslant L \leqslant 80$. The solid line is a power-law fit for large l. The inset shows the saturated mean square domain size $R^2_s(L) \sim L^2$. (b) The mean square domain size $R^2(l)$ for the PBA model as a function of the layer number l for $20 \leqslant L \leqslant 60$. The two solid lines are power-law fits to data; $R^2(l) \sim l^{0.67}$ for $l \leqslant 50$, and $R^2(l) \sim l^{0.21}$ for $l \geqslant 50$. In both figures $k_BT/J = 1.0$, $F = 1$ ML s^{-1}, and $D = 80$ s^{-1}/site.

The power-law behaviour of $R(l) \sim l^{1/2}$ agrees very well with the results of the NCOP domain coarsening at order–disorder phase transitions if one regards l as time t. The saturated domain size $R_s(L) \sim L$, shown in the inset of figure 3(a), is due to finite-size effects. Equation (13) indicates that for large L and l, the behaviour of $R(l)$ with $z_D = 2$ is very similar to that described by equation (1), $R(t) \sim t^{1/2}$ for the NCOP domain growth. For the PBA model, $R^2(l)$ also shows a power-law behaviour with values of exponents different from that of the restricted PBA model. There is a crossover: approximately, $R(l) \sim l^{1/3}$ for $l \leqslant 50$, and $R(l) \sim l^{0.11}$ for $l \geqslant 50$. Although at early stages, the exponent $1/3$ happens to be equal to that of the case of COP domain growth, a slight change in growth conditions (e.g. the ratio of diffusion to flux and temperature) and interactions yields a different value of the exponent and the crossover layer number.

At late times, the domain growth process is quite suppressed by large APBs present on the surface mainly due to the lack of enough surface diffusion, and this may lead to a slow growth of domain size for large l in the PBA model. Since the surface free energy of APBs is higher than that of ordered domains, the ordering process proceeds mainly on the existing ordered domain on the surface. However, due to a growing roughness of the surface as growth proceeds, a particle may not find a site which minimizes the surface free energy.

4.3. Binary alloy growth: surface roughening

The saturated mean square interfacial width for the restricted PBA model is shown in the inset of figure 4(a), $w_s^2(L) \sim \log L$, implying $\zeta = 0$. The behaviour of $w_s(L)$ agrees with the experimental results for surface roughening in $Si_{1-x}Ge_x$ film growth on Si at large length scales [16], and is consistent with the theoretical description of the EW equation with the scaling behaviour $w_s^2(L) \simeq (D/2\pi\nu) \log L$ [17, 33]. The decrease in the interfacial width for small system sizes, shown in figure 4(a), is a finite-size effect due to the A-type substrate and the strong Ising type of interactions in the model, which disappears in a large system size: see the result for $L = 160$. The dynamic exponent $\gamma = 2.0 \pm 0.1$ is obtained from the saturated structure factor $S(k) \sim k^{-\gamma}$ which is not shown here to avoid overcrowding of the figures. We have also obtained an excellent scaling collapse for the structure factor $S(k, t)$ with $z = \gamma$ using the scaling function given in equation (5). The exponents obtained obey the hyperscaling relation $z = 2\zeta + d'$. The growth exponent $\beta = 0$ with $w(t) \sim \log t$ at late stages, as shown in figure 4(a). This behaviour is the same as that of the monatomic UDP model. It seems that the height restriction imposed on the restricted PBA model and the ordering process on the surface induce a downhill surface current, and this again leads to EW behaviour.

For the PBA model, the interfacial width, shown in the inset of figure 4(b), does not show any power-law behaviour, but $\log[w(L, t)] - w_I \sim t^{\beta}$ with $\beta = 0.222$, i.e. $w(t) \sim \exp[t^{\beta}]$. A similar behaviour is also obtained for the film of the same PBA model grown on a perfect ordered substrate. We have found an exponential system size dependence of the saturated width, $w_s(L) \sim e^{aL}$ with $a = 0.042$. Although the exponential growth of the interfacial width, often called rapid roughening, has been observed in several semiconductor surfaces at low temperatures [34], the detailed growth mechanism leading to the behaviour is still unclear to us. A careful examination of horizontal and vertical cross sections of a grown film and top views of the surface at different times for the PBA model shows that the APBs are located at a lower height on the surface. As seen in figure 3(b), a slow growth of domain size after $l \geqslant 50$ implies that the density of the APB on the surface is large at late times. Since, in the UDP model, a particle tries to increase its binding energy, the particle thus avoids a site at a lower height if there is an APB near the site, due to the high surface free energy of the APB, and prefers to move a site at an ordered cluster that is quite localized between the APBs. However,

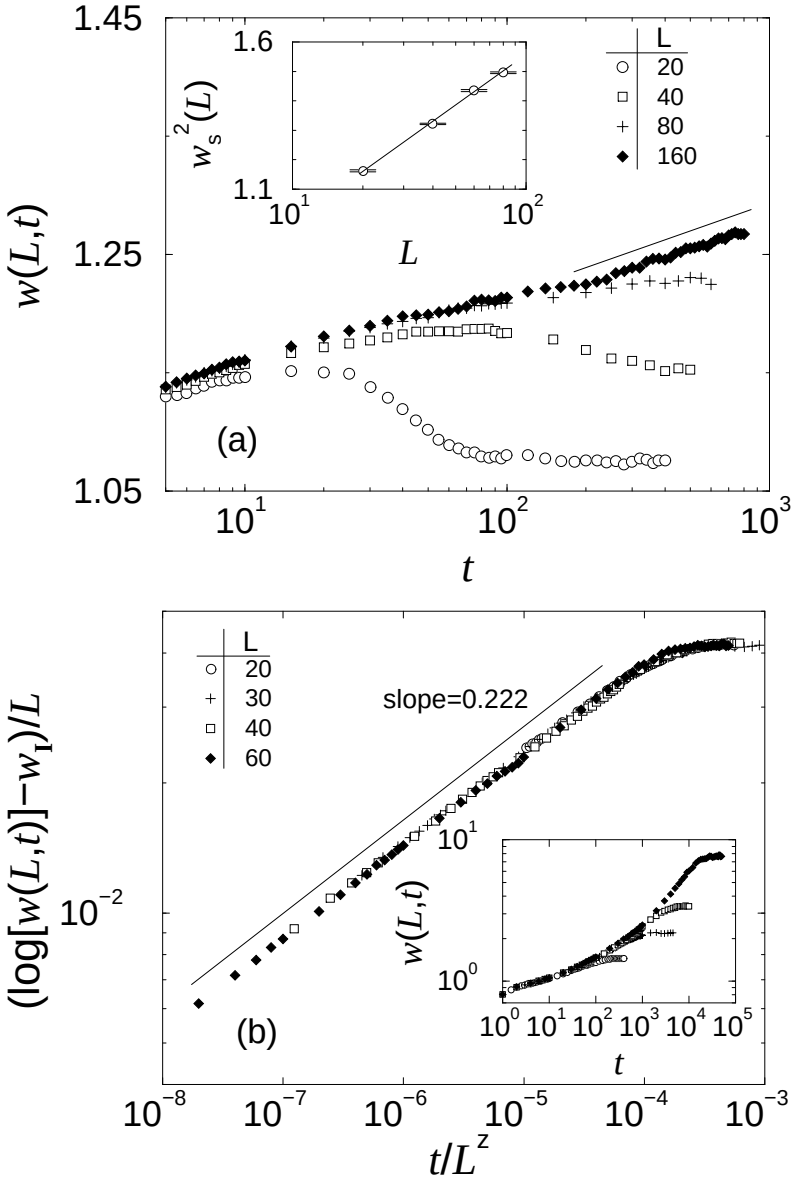

Figure 4. (a) The interfacial width as functions of system size L and time t for the restricted PBA model. The saturated interfacial width $w_s^2(L) \sim \log L$ is shown in the inset. (b) The scaled interfacial width for the PBA model. The inset shows the interfacial width for the PBA model. The saturated interfacial width $w_s(L) = e^{aL+w_I}$ with $a = 0.042 \pm 0.001$ and $w_I = -0.465$. Here $z = 4.5 \pm 0.2$ has been used for the scaling. In both figures $k_B T/J = 1.0$, $F = 1$ ML s^{-1}, and $D = 80$ s^{-1}/site.

this rough argument does not explain the exponential behaviour of the saturated interfacial width and we have not found a theoretical continuum growth equation which explains the unusual growth of surface fluctuations for the PBA model.

As shown in the inset of figure 5, the saturated interfacial width for the RBA model is $w_s(L) \sim L$ with $\zeta = 1$. This behaviour is the same as that of the monatomic UDR model;

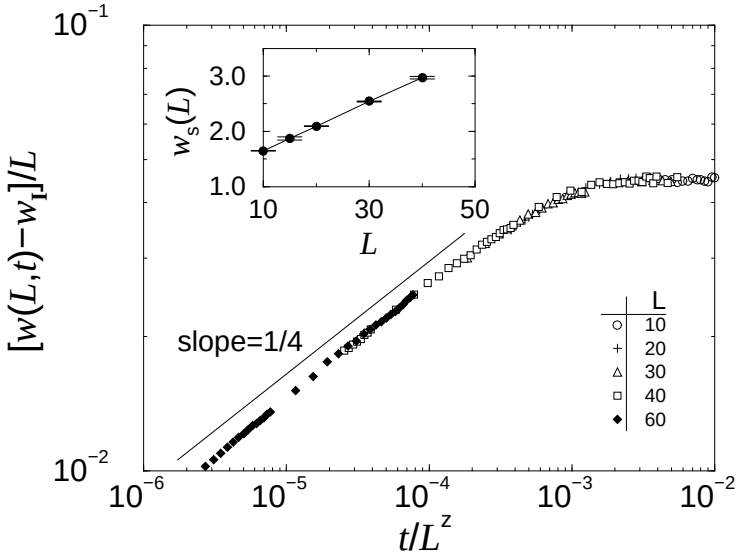

Figure 5. (a) The scaled interfacial width for the RBA model with $k_BT/J = 1.0$, $F = 1$ ML s^{-1}, and $D = 80$ s^{-1}/site. Here, $w_I = 1.2$ and $z = 4$ have been used. The inset shows the saturated interfacial width $w_s(L) = aL + w_I$ with $a = 0.044 \pm 0.001$ and $w_I = 1.22 \pm 0.02$.

unlike the UDP model, binary alloy and monatomic UDR models are both well described by the MH equation at the temperature.

For the scaling shown in figure 5, $z = 4$ has been used. Figure 5 indicates that for $1 \ll t \ll L^z$, $w(L,t) - w_I \sim t^{1/4}$, and at very late times and for large L, β approaches the asymptotic value 1/4. Since the domain size $R(l)$ is not a self-averaging quantity, its calculation requires a quite large number of independent runs. The domain size $R(l)$ for the RBA model has also been calculated for $L \leqslant 40$, but is not shown here due to the modest statistical averaging. However, we do not find any power-law behaviour in $R(l)$ within error bars.

At this moment, theoretical continuum equations available for the growth by MBE are based on homoepitaxial film growth. Thus the effect of the substrate and inhomogeneous interactions between different kinds of particle on the surface roughening is less clear, and further studies are needed to produce a better understanding of binary mixture film growth.

5. Conclusions

In this paper we have considered multilayer $A_{0.5}B_{0.5}$ film growth on an A-type substrate and homoepitaxial film growth by molecular beam epitaxy simulations. This study encompassed both growth-induced domain coarsening and noise-induced surface roughening. Our models include the random deposition of particles and surface diffusion, which are the essential features of molecular beam epitaxy. The results of binary alloy growth models are compared to those of the monatomic UDP and UDR models.

It turns out that in the monatomic UDR and RBA models, surface diffusion is the main relaxation process at temperature, and the growth is well explained by the Mullins–Herring equation with a linear size dependence of the saturated width in a steady state. On the other hand, in the monatomic UDP and restricted PBA models, surface tension is a driving force

which governs the growth of films and leads to a logarithmic growth of the interfacial width. Thus, the UDP and restricted PBA models belong to the Edwards–Wilkinson universality class. The behaviour of the interfacial width for the PBA model is quite different from other models considered here, and there is no corresponding continuum growth equation which explains the unusual growth of surface fluctuations.

The antiphase boundaries initially induced by the substrate and the random deposition of a binary mixture are eliminated by the coarsening process, leading to a power-law growth of the domain size as films grow. It seems that the exponent characterizing domain growth depends on the models and growth conditions.

Simulation results of our binary alloy models indicate the interplay between the domain growth and the surface roughening, but more extensive studies are needed to understand non-equilibrium domain growth by molecular beam epitaxy and the coupling between growth-induced pattern formation and growth-induced surface roughening.

Acknowledgment

The work was supported by the National Science Foundation under Grant No DMR-9727714.

References

[1] Farrow R F C (ed) 1995 *Molecular Beam Epitaxy Application to Key Materials* (Englewood Cliffs, NJ: Noyes) and references therein
[2] Family F and Vicsek T 1991 *Dynamics of Fractal Surfaces* (Singapore: World Scientific)
Barabasi A-L and Stanley H E 1995 *Fractal Concepts in Surface Growth* (Cambridge: Cambridge University Press) and references therein
[3] LeGoues F K, Kesan V P and Iyer S S 1990 *Phys. Rev. Lett.* **64** 40
Kesan V P, LeGoues F K and Iyer S S 1992 *Phys. Rev.* B **46** 1576
[4] Kuan T S, Kuech T F, Wang W I and Wilkie E L 1985 *Phys. Rev. Lett.* **54** 201
[5] Philips B A, Kamiya I, Hingerl K, Florez L T, Aspnes D E, Mahajan S and Harbison J P 1995 *Phys. Rev. Lett.* **74** 3640
[6] Bellon P, Chevalier J P, Augarde E, Andre J P and Martin G P 1989 *J. Appl. Phys.* **66** 2388
[7] Gomyo A, Suzuki T and Iijima S 1988 *Phys. Rev. Lett.* **60** 2645
[8] Ourmazd A and Bean J C 1985 *Phys. Rev. Lett.* **55** 765
LeGoues F K, Kesan V P, Iyer S S, Tersoff J and Tromp R 1990 *Phys. Rev. Lett.* **64** 2038
[9] Cao D S, Kimball A W, Chen G S, Fry K L and Stringfellow G B 1989 *J. Appl. Phys.* **66** 5384
[10] McRae E G and Malic R A 1990 *Phys. Rev. Lett.* **65** 737
[11] Park B, Stephenson G B, Allen S M and Ludwig K F Jr 1992 *Phys. Rev. Lett.* **68** 1742
[12] Ikarashi N, Akimoto K, Tatsumi T and Ishida K 1994 *Phys. Rev. Lett.* **72** 3198
[13] Smith J R Jr and Zangwill A 1996 *Phys. Rev. Lett.* **76** 2097
[14] Zangwill A 1996 *J. Cryst. Growth* **163** 8
[15] Kotrla M and Predota M 1997 *Europhys. Lett.* **39** 251
Kotrla M, Slanina F and Predota M 1998 *Phys. Rev.* B **58** 10 003
[16] Mou C-Y and Hsu J W P 1996 *Phys. Rev.* B **53** R7610
[17] Edwards S F and Wilkinson D R 1982 *Proc. R. Soc.* A **381** 17
[18] Hohenberg P C and Halperin B I 1977 *Rev. Mod. Phys.* **49** 435
[19] Bray A J 1994 *Adv. Phys.* **43** 357 and references therein
[20] Wang G-C and Lu T-M 1983 *Phys. Rev. Lett.* **50** 2014
[21] Sadiq A and Binder K 1984 *J. Stat. Phys.* **35** 517
Gawlinski E T, Grant M, Gunton J D and Kaski K 1985 *Phys. Rev.* B **31** 281
[22] Family F and Vicsek T 1985 *J. Phys. A: Math. Gen.* **18** L75
[23] Siegert M and Plischke M 1994 *Phys. Rev.* E **50** 917
[24] Herring C 1950 *J. Appl. Phys.* **21** 301
Mullins W W 1957 *J. Appl. Phys.* **28** 333
[25] Kim J M and Das Sarma S 1994 *Phys. Rev. Lett.* **72** 2903

[26] Wolf D F and Villain J 1990 *Europhys. Lett.* **13** 389
[27] Pal S and Landau D P 1994 *Phys. Rev.* B **49** 10 597
Landau D P and Pal S 1996 *Langmuir* **12** 29
Landau D P and Pal S 1996 *Thin Solid Films* **272** 184
[28] Saito Y 1981 *J. Chem. Phys.* **74** 713
Saito Y and Müller-Krumbhaar H 1981 *J. Chem. Phys.* **74** 721
[29] Shim Y, Landau D P and Pal S 1998 *Phys. Rev.* E **58** 7571
[30] Allen S M and Cahn J W 1979 *Acta Metallurgica* **27** 1085
[31] Ishimaru M, Matsumura S, Kuwano N and Oki K 1995 *Phys. Rev.* B **51** 9707
[32] Matsumura S, Takano K, Kuwano N and Oki K 1991 *J. Cryst. Growth* **115** 194
[33] Nattermann T and Tang L-H 1992 *Phys. Rev.* A **45** 7156
[34] Krug J 1997 *Adv. Phys.* **46** 139 and references therein